Biochimica et Biophysica Acta 1798 (2010) 1689–1697

Contents lists available at ScienceDirect

Biochimica et Biophysica Acta

journal homepage: www.elsevier.com/locate/bbamem

Electrophoretic mobility of sarcoplasmic reticulum vesicles is determined by amino acids of A + P + N domains of Ca^{2+}–ATPase

Pavel Smejtek *, Laura E. Satterfield, Robert C. Word, Jonathan J. Abramson

Department of Physics and Molecular Biosciences Group, Portland State University, Portland, Oregon 97207-0751, USA

ARTICLE INFO

Article history:
Received 10 December 2009
Received in revised form 19 April 2010
Accepted 4 May 2010
Available online 12 May 2010

Keywords:
Electrophoretic mobility
Sarcoplasmic reticulum
Photoelectron microscopy
Size distribution
Ca2+–ATPase
Calcium pump
Zeta potential
pH dependence
Cytoplasmic domain
SR vesicle

ABSTRACT

Establishing the origin of electrophoretic mobility of sarcoplasmic reticulum (SR) vesicles is the primary goal of this work. It was found that the electrophoretic mobility originates from ionizable amino acids of cytoplasmic domains of the Ca^{2+}–ATPase, the calcium pump of SR. The mobility was measured at pH 4.0, 4.7, 5.0, 6.0, 7.5, and 9.0 in the region of ionic strength from 0.05 to 0.2 M. Mobility measurements were supplemented by studies of SR vesicles by photoelectron microscopy. The median diameter of SR vesicles was 260 nm. Ca^{2+}–ATPases were not resolved. The mobility data were standardized by interpolation to a reference ionic strength of 0.1 M. The mobility of the SR vesicles is determined by the charge of the Ca^{2+}–ATPase. It is due to the ionizable amino acids selected from the amino acid sequence of SERCA1a Ca^{2+}–ATPase. The pH dependence of charge residing in various domains of Ca^{2+}–ATPase was computed using pKa values in free water. The charge correlated with measured mobility. It was shown that a linear relationship exists between the mobility of the SR vesicles, μ, and the total computed charge, Q, on three cytoplasmic domains of Ca^{2+}–ATPase: A, P, and N. It is given by $\mu = \alpha + \beta Q$ where the fitted values $\beta = (0.043 \pm 0.002) \times 10^{-8}\ m^2\ V^{-1}\ s^{-1}\ e^{-1}$ and $\alpha = (0.16 \pm 0.02) \times 10^{-8}\ m^2\ V^{-1}\ s^{-1}$. Since β and α values do not change from pH 4 to pH 9, one concludes that the hydrodynamic friction of the cytoplasmic domains of SR is independent of their charge.

1. Introduction and background

Particle electrophoresis is now an established experimental method for the study of the electrostatic and hydrodynamic properties of colloids, whose sizes range from tens of nanometers to several micrometers. It has been a valuable tool to characterize the surface of particles in science, medicine, and technology. Furthermore, the dependence of electrophoretic mobility on pH makes it possible to establish the pH dependence of surface charge and thus it provides insight into its origin. Notable are studies of red blood cells that established a three layer model of red blood cell surface [1]. The authors found that the charge of the innermost layer becomes positive at low pH due to the protonation of amino acids of surface glycoproteins. This charge compensates the negative charge of the outer surface layer that is pH-independent. Another pioneering work that was also based on measurements of pH dependence of mobility [2] was the study of *Escherichia coli*, a bacterium covered with lipopolysaccharide layer and of *Staphylococcus aureus*, another bacterium covered with peptidoglycan layer. Interfacial properties of bacteria play important, but not well understood, roles in the mechanism of interaction with their environments. Recent studies [3] examined the electrostatic properties of the charge-regulated bacterial surface of *E. coli* and *Bacillus brevis*.

Liposomes continue to have a prominent role as models for a great variety of biological membranes [4] and for improvements of theoretical models of electrophoretic mobility [5]. Initially the theories of electrophoretic mobility were developed for a class of "hard particles," rigid spheres with smooth surfaces. These studies were based on Helmholtz–Smoluchowski theory [6] and later expanded to the "standard electrokinetic model" that accounts for the effect of particle size [7,8]. The other class of particles is known as "soft particles". Soft particles have rigid cores covered by charged or uncharged polymer layers. Ohshima [5] is credited for his major contributions to theoretical and experimental advances in studies of soft particles and for numerous analytical solutions of electrophoretic mobility models. Kuo [9] worked out a number of theoretical problems on mobility of particles with complex surface properties. An excellent overview of electrokinetic methods, including practical recommendations, was recently produced by the Physical and Biophysical Chemistry Division of IUPAC [10].

It is recognized that a description of soft particles in terms of a homogeneous surface layer of constant thickness may not be adequate. It has been shown that polyethylene glycol chains anchored in a lipid bilayer exist in various conformations, from mushroom-like to brush-like, depending on their surface density. These studies indicate the need to introduce statistical mechanics into the electrophoretic mobility theory of particles with complex surfaces [11,12].

* Corresponding author.
E-mail address: smejtekp@pdx.edu (P. Smejtek).

0005-2736/$ – see front matter © 2010 Elsevier B.V. All rights reserved.
doi:10.1016/j.bbamem.2010.05.003

There are a number of proposals that further generalize the standard electrokinetic model. The most recent one [13] is based on the assumption that a very thin layer of mobile ions exists at the particle surface whose density is not determined by the conventional diffuse layer model but by other mechanisms. In contrast to the standard model, in the new generalized model the fluid (water) is allowed to flow along the particle surface. The major impact of this proposal is that the magnitude of mobility can be higher than that predicted from the standard electrokinetic model.

Another important recent development is that some biological particles may not be rigid. In the presence of an external electric field used in an electrophoretic experiment, particles can deform due to fluid flow and become ellipsoidal. Furthermore, their surface charges may redistribute. The change in shape of biological particles was demonstrated by controlling liposome rigidity via cholesterol content. Less rigid liposomes exhibited greater mobility because they became more elongated along the direction of motion [14,15]. These effects are not included in the standard model and require special treatment.

The present study is focused on the origin of electrophoretic mobility of sarcoplasmic reticulum (SR) vesicles. These vesicles have very different surface properties compared to bacteria. The lipopolysaccharide (Gram-negative bacteria) or the peptidoglycan (Gram-positive bacteria) layers are absent on the sarcoplasmic reticulum membrane. Instead the SR membrane has Ca^{2+}–ATPases incorporated into the bilayer. Ca^{2+}–ATPase is an ATP-driven calcium pump.

Understanding the relationship between the electrokinetic properties and the surface properties of sarcoplasmic reticulum requires bringing together two fields of study. The first is the structure of the Ca^{2+}–ATPase protein and the other is the electrophoretic mobility of colloidal particles. On one hand, the Ca^{2+}–ATPase is one of the most extensively studied membrane enzymes [16] but, on the other hand, the origin of electrokinetic properties of the SR membrane remains unknown.

The amount of published research on electrokinetic properties of SR membrane is rather small. The lack of progress is most likely caused by the complex structure and, consequently, electrokinetic properties of the SR surface that were not interpretable. In retrospect, the electrophoretic mobility data obtained already in the 1980s suggested that the electrokinetic properties of SR are complex [17]. The most notable contributions are the works of Arrio et al. who measured the mobility of vesicles prepared from native SR and compared the results with the mobility of SR vesicles reconstituted with uncharged and charged lipids [18]. The mobility results were later rationalized in a computational study based on numerical solution of one-dimensional Poisson–Boltzmann and Navier–Stokes equations [19]. However, all these earlier studies were done at a single pH value, and thus do not provide insight into the origin of surface charge of the SR membrane.

A schematic diagram of Ca^{2+}–ATPase architecture is depicted in Fig. 1. The molecule, with bound Ca^{2+}, can be enclosed in a box with dimensions of 10 nm × 8 nm × 14 nm [20]. The outer surface of SR vesicles is covered by dense arrays of Ca^{2+}–ATPases. From optical diffraction analysis of electron micrographs of freeze-fractured SR vesicles it was found that Ca^{2+} pumps are organized into arrays resembling hexagonal or tetragonal lattices [21]. For tetragonal arrays the dimensions of unit cell are 11.7 ± 0.7 nm in the *a*-direction and 10.5 ± 0.5 nm in the *b*-direction with unit cell area of 123 ± 9 nm^2. For hexagonal arrays the unit cell defined as body-centered rectangular cell had a repeat distance of 13.12 nm, and unit cell area per freeze-fractured particle (Ca^{2+} pump) of 130 ± 10 nm^2. Thus the surface density of Ca pumps is about 8.15×10^{15} m^{-2} (8150 pumps per μm^2) for tetragonal array and 7.71×10^{15} m^{-2} (7710 pumps per μm^2) for hexagonal array.

In Fig. 1 the transmembrane domains are designated by the letter M, and the large structures above the lipid membrane surface are the cytoplasmic domains: A (actuator), P (phosphorylation), and N (nucleotide binding).

The origin of electrophoretic mobility of sarcoplasmic reticulum vesicles is the primary goal of this project. We measured their electrophoretic mobility as a function of ionic strength for a series of pH values from pH 4 to pH 9. We show that the pH dependence of mobility has a unique dependence on the electric charge carried by three cytoplasmic domains of Ca^{2+}–ATPase designated as A, P and N. The total charge of A + P + N domains of the Ca^{2+}–ATPase determines the electrophoretic mobility of SR vesicles.

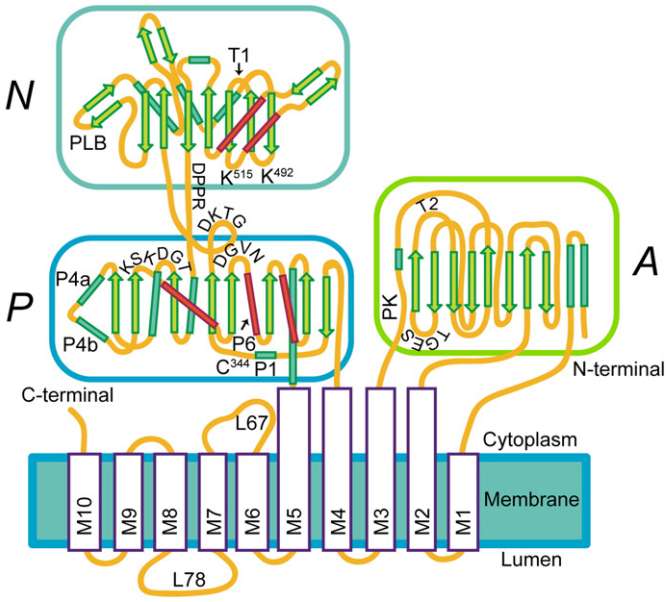

Fig. 1. Topology of calcium pump of SR membrane illustrating the A, P, N cytoplasmic domains, and transmembrane helices M. Not to scale (adapted from Stokes and Green [35]).

2. Materials and methods

2.1. Suspensions of sarcoplasmic reticulum vesicles

SR vesicles were isolated from rabbit fast twitch skeletal muscle by the method of MacLennan [22]. Samples were stored in liquid nitrogen. The vesicles were physiologically active, they pumped and released calcium. SR vesicles stored in liquid N_2 were functionally indistinguishable from freshly prepared samples. The protein concentration was determined by absorption spectroscopy [23]. To prepare samples for mobility measurements SR vesicles were diluted down to 0.08 g/L in salt solutions of different ionic strength and pH.

Electrophoretic mobilities of vesicles suspended in aqueous solution were measured as a function of ionic strength at six different pH values (4.0, 4.7, 5.0, 6.0, 7.5, and 9.0). For each pH value, a stock solution was made with buffer concentration equal to 10 mM. Sodium acetate was used for pH 4, 4.7, and 5. MES was used for pH 6, HEPES sodium salt for pH 7.5, and CHES for pH 9. Buffer solutions were titrated to the appropriate pH using HCl or KOH. Salt stock solutions were made using NaCl crystals dissolved in the buffer solution. The pH of the salt stocks was monitored and adjusted as needed. Salt dilutions were made by mixing buffer solutions and salt stocks.

2.2. Photoelectron microscopy

Photoelectron microscopy was used with two goals in mind: (a) to image the surface layer consisting of Ca^{2+}–ATPases, and (b) to measure the size distribution of SR vesicles to be used in standard electrokinetic model [8]. This study was done with Portland State University's aberration-corrected photoelectron microscope (CPEM). Images in this microscope are produced by photoelectrons emitted from the surface of SR vesicles when illuminated with UV light produced by a 244-nm argon laser. The SR suspension prepared at pH 7 had a protein concentration of 27.0 g/L. This preparation of SR

vesicles was diluted by a factor 10,000:1 with distilled water at pH 7 and deposited on chromium oxide-coated glass to generate high contrast images. The surface layer consisting of Ca^{2+}–ATPases was not observed. It was assumed that the flattened desiccated vesicles were elliptical and that their original shapes were spheres. The surface areas of desiccated and original vesicles were assumed to be equal. The median diameter of SR vesicles was 260 nm (Fig. 2). This is in good agreement with previous measurements made with freeze-fracture electron microscopy [24].

2.3. Particle electrophoresis

Electrophoretic mobility of SR vesicles was measured at 25 °C using an electrophoretic mobility analyzer DELSA 440 (Beckman-Coulter, Fullerton, CA, USA). The mobilities were obtained from simultaneous measurements of light scattered at angles 8.6°, 17.1°, 25.6°, and 34.2° using instrument settings recommended by the manufacturer.

2.4. Experimental design and approach to data analysis: dependence of mobility of SR vesicles on pH and ionic strength

The objective of the mobility experiments is to obtain data on the dependence of mobility on the pH under standardized conditions so that the mobility data obtained for different pH can be compared. To that effect, we have measured the mobility within a region of moderate to high ionic strength, from about 0.05 to 0.2 M, as a function of pH. The pH values were 4.0, 4.7, 5.0, 6.0, 7.5, and 9.0 with uncertainty of about 0.1 pH units. pH values of mobility samples were checked after the mobility measurement. For some pH values it was not possible to obtain accurate data in full range of ionic strengths because of instrumental limitations at the high end of the ionic strength range, when the mobility values are too close to zero. The reason is that the mobility analyzer DELSA 440 employs the concept of frequency shifts of light scattered from the vesicles moving in the applied electric field. At high ionic strength the frequency shifts become too small and erratic resulting in unreliable mobility data.

2.5. General features of mobility of SR vesicles

We have measured the dependence of mobility of SR vesicles on ionic strength of monovalent salt solution as a function of pH of vesicle suspension. It is useful to correlate the mobility data with the methods used in their analysis using an example. Fig. 3 compares three approaches to analysis of mobility vs. ionic strength at pH 4—an empirical linear least square fit, a nonlinear least square fit of the Helmholtz–Smoluchowski model (broken curve), and the Standard Electrokinetic Model computed using analytical formulation by Ohshima, Healy and White, Eq. (3.184) [5] (solid curve). The mobility computed from the Standard Electrokinetic Model was obtained for the same value of charge density as that for the Helmholtz–Smoluchowski model (9.93×10^{-3} C-m^{-2} which is the least square fit value for the Helmholtz–Smoluchowski model).

The notable feature of mobility of SR vesicles is that (a) neither the Helmholtz–Smoluchowski nor the Standard Electrokinetic Model are fully consistent with the experimental dependence of mobility on ionic strength, and (b) that the simple Helmholtz–Smoluchowski theory is an adequate approximation of the Standard Electrokinetic Model when analyzing the experimental results. There is no mobility model available in the literature that would be applicable to the surface of SR membrane.

The quantity κa, known as the product of the reciprocal Debye length of diffuse space charge layer surrounding the vesicle, κ, and the vesicle radius, a, plays an important role in condition of applicability of Helmholtz–Smoluchowski theory and in applicability of analytical formulation of Standard Electrokinetic Model [5,25]. The reciprocal Debye length is equal to

$$\kappa = \left(\frac{2F^2(1000c_0)}{\varepsilon\varepsilon_0 RT}\right)^{1/2}. \quad (1)$$

The quantity c_0 is the molar concentration of the 1:1 electrolyte used in the study. c_0 also determines the ionic strength of the suspension. Other quantities have their usual meaning.

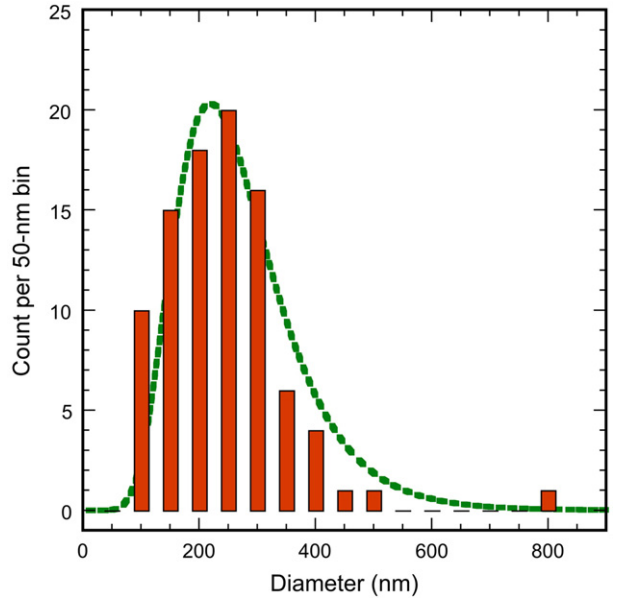

Fig. 2. Size distribution of SR vesicles. The dashed curve represents a best-fit of the log-normal distribution.

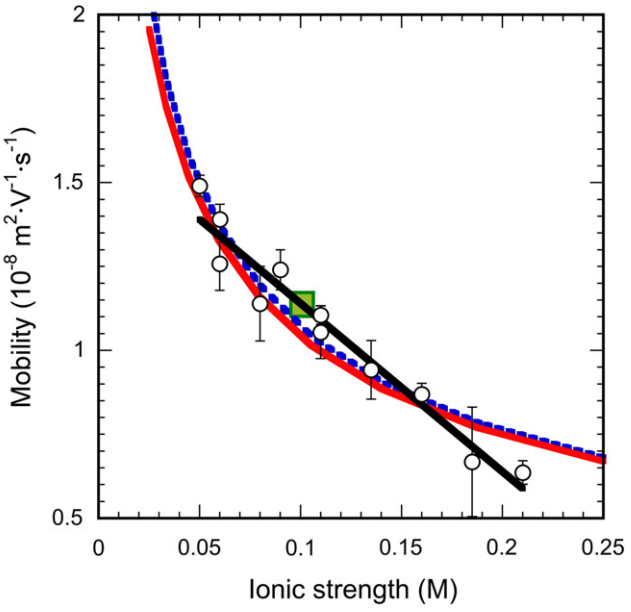

Fig. 3. Illustration of three approaches to the analysis of mobility using data for pH 4: (1) empirical linear approximation and (2) nonlinear approximation by Helmholtz–Smoluchowski model (broken curve) and (3) the mobility predicted from the Standard Electrokinetic Model (solid curve). According to method (1) the data are interpolated by a linear function to obtain a representative value of mobility for ionic strength of 0.1 M (shown by filled square). This mobility value is then used to obtain the apparent ζ-potential and the apparent surface charge density σ_{Lin} at a given pH. According to method (2) the apparent surface charge density $\sigma_{HS}=9.93\times10^{-3}$ C-m^{-2} is found from the least squares fit of the mobility data to Helmholtz–Smoluchowski model. The broken curve illustrates the dependence of mobility on ionic strength predicted from the Helmholtz–Smoluchowski model. (3) The solid curve shows the mobility predicted from the analytic form of Standard Electrokinetic Model, Eq. (3.184) in reference [5]. It was calculated for $\sigma_{HS}=9.93\times10^{-3}$ C-m^{-2} and for vesicle radius $a=105$ nm (corresponding to the maximum in vesicle size distribution shown in Fig. 2).

The range of κa corresponding to ionic strengths of data shown in Fig. 3 is $77<\kappa a<158$. It was computed for vesicle radius $a=105$ nm. This value of vesicle radius corresponds to the peak in SR vesicle size distribution shown in Fig. 2.

It was concluded from the close agreement between the mobility predicted from the Standard Electrokinetic Model and the Helmholtz–Smoluchowski model (Fig. 3) that considering the scatter of experimental mobility data it is valid to use the mobility obtained from the Smoluchowski equation (Eq. (2)) for further analysis of experimental data. In the Smoluchowski equation

$$\mu = \frac{\varepsilon\varepsilon_0}{\eta}\zeta \tag{2}$$

μ represents the mobility, and ζ the apparent electrokinetic potential or apparent ζ-potential.

For hard and smooth particles, the ζ-potential is the electrostatic potential at the surface of shear, which is inside the diffuse layer. At this surface water begins to move freely relative to the surface of the particle. The shear surface loses its physical meaning for particles whose surface is covered by water permeable surface layer, like the layer of Ca^{2+}–ATPases embedded in the bilayer. This layer is expected to exert hydrodynamic drag on the SR vesicle and to reduce mobility. In contrast to hard particles there is no sharp boundary in the velocity of flow of water relative to the surface of the particle, rather a fuzzy region inside the surface layer where the velocity markedly increases. Cohen and Khorosheva [26] presented physically meaningful definition of the apparent ζ-potential and apparent shear surface for large vesicles ($\kappa a>>1$) covered with uncharged polymer layer.

In the present work the ζ-potential obtained from Eq. (2) is also referred to as apparent ζ-potential even though the surface layer of SR vesicles is different from the uncharged polymer layer used for the definition of apparent electrokinetic quantities. Furthermore, no distinction is made between the surface potential and the ζ-potential. This is necessary since there is no adequate model for electrostatics and hydrodynamics of SR.

2.6. Surface charge density and the ζ-potential

The apparent ζ-potential obtained from Eq. (2) is also used to determine the apparent surface charge density σ. It follows from close agreement of mobility obtained from the Standard Electrokinetic Model and the Helmholtz–Smoluchowski model that in the range of ionic strength used in the study, and particularly for ionic strength of 0.1 M, that a small segment of vesicle surface can be regarded as planar. In this case the apparent surface charge density is related to the apparent ζ-potential according to

$$\sigma = [8\varepsilon\varepsilon_0(1000c_0)]^{\frac{1}{2}}\sinh(F\zeta/2RT). \tag{3}$$

This equation is known as the Gouy equation. It is applicable to symmetric 1:1 electrolytes as used in our experiments. The quantity c_0 is the molar concentration of the 1:1 electrolyte. For low potentials, $F\zeta/2RT \ll 1$, a condition applicable to our experimental data, Eq. (3) becomes

$$\sigma = \varepsilon\varepsilon_0\kappa\zeta. \tag{3a}$$

3. Results and discussion

3.1. Electrophoretic mobility of SR vesicles, apparent ζ-potential and apparent surface charge densities

Before analyzing the pH dependence of mobility, the mobility data at the high end of the ionic strength range were omitted since very small mobilities are exceedingly difficult to measure and are therefore highly unreliable. Mobility data at each pH were analyzed two ways: (1) for each pH value, the measured mobilities were interpolated to ionic strength of 0.1 M using an empirically selected linear interpolation function. This interpolation uses a larger number of measured mobility points within the ionic strength range that reduces the error of mobility at the reference ionic strength of 0.1 M and reduces the effect of nonrandom errors. (2) For each pH value, the mobilities, measured as a function of ionic strength, were fit using the Helmholtz–Smoluchowski model. Using this approach we obtained a least squares fit value of an apparent surface charge density at each pH.

Using the above two approaches we obtained two sets of apparent surface charge densities: (1) σ_{Lin} from the linear interpolation to ionic strength 0.1 M, and (2) σ_{HS} from the least squares fit of mobility data to Helmholtz–Smoluchowski model.

The experimental results of mobility measurements as a function of ionic strength for pH 4.0, 4.7, 5.0, 6.0, 7.5 and 9.0 are presented in Fig. 4A. Also shown are the results of data treatment by linear interpolation and by the least squares fit of mobility data to Helmholtz–Smoluchowski model.

The dependence of apparent charge densities obtained from the linear interpolation of mobilities and the least squares fit of Helmholtz–Smoluchowski model to all mobility data at a given pH are shown in Fig. 4B. The plot shows that the results of both analytical approaches produce very similar charge densities of SR vesicles.

In order to objectively establish whether the linear or nonlinear treatment of the experimental data is more appropriate we estimated the goodness of fits by calculating the variance of the fit, s^2 [27].

The values of variances of the fit, s^2, were calculated for all individual pH data sets for the linear fit and nonlinear Helmholtz–Smoluchowski models, and the individual s^2 were added. It was found that overall the dependence of mobility of SR vesicles on ionic strength is represented better by the linear approximation than by the Helmholtz–Smoluchowski model. The values of variances were $s^2(\mathrm{total})_{\mathrm{Lin}}=0.018$ whereas $s^2(\mathrm{total})_{\mathrm{HS}}=0.033$.

In view of the absence of a mobility model suitable to describe the dependence of mobility of SR vesicles on ionic strength we used a reference ionic strength of 0.1 M in the analysis of experimental data. The apparent ζ-potential and apparent surface charge density at the reference ionic strength were obtained from the Helmholtz–Smoluchowski model.

The apparent charge density of SR vesicles depends on bulk pH as illustrated by data in Fig. 4B. Since the protonation/deprotonation is taking place at the charged surface of SR we take into the account that the interfacial concentration $[H^+]_{\mathrm{if}}$ is different from that in the bulk aqueous phase $[H^+]$,

$$\left[H^+\right]_{\mathrm{if}} = \left[H^+\right]\exp(-F\zeta/RT). \tag{4}$$

The bulk pH and the interfacial pH, the measured mobility μ, the apparent ζ-potential and the apparent surface charge density σ are summarized in Table 1.

At physiological pH the mobility, the apparent ζ-potential and the apparent surface charge density σ are negative due to the prevailing negative charge below the diffuse layer. We found the sign reversal of mobility at bulk pH 5.6. At low pH (pH<5.6) the quantities μ, ζ, and σ are positive indicating the dominance of the positive surface charge of the SR membrane. Qualitatively similar properties were found for human erythrocytes [1]. The dependence of experimental mobility on interfacial pH is illustrated in Fig. 5.

3.2. Electric charge of SR membrane and its dependence on pH

The electric charge of the SR vesicle is the primary quantity determining its electrophoretic mobility. Three major charge contributors are Ca^{2+}–ATPase—the dominant SR protein, charged lipids, and sialic acid residues. It will be shown in Section 3.4 that the electrophoretic mobility is determined by charges residing on the Ca^{2+}–ATPase.

Charge of Ca^{+2}-ATPase is due to ionizable amino acids. Since the architecture of Ca^{2+}–ATPase is complex, as shown in Fig. 1, it is not a

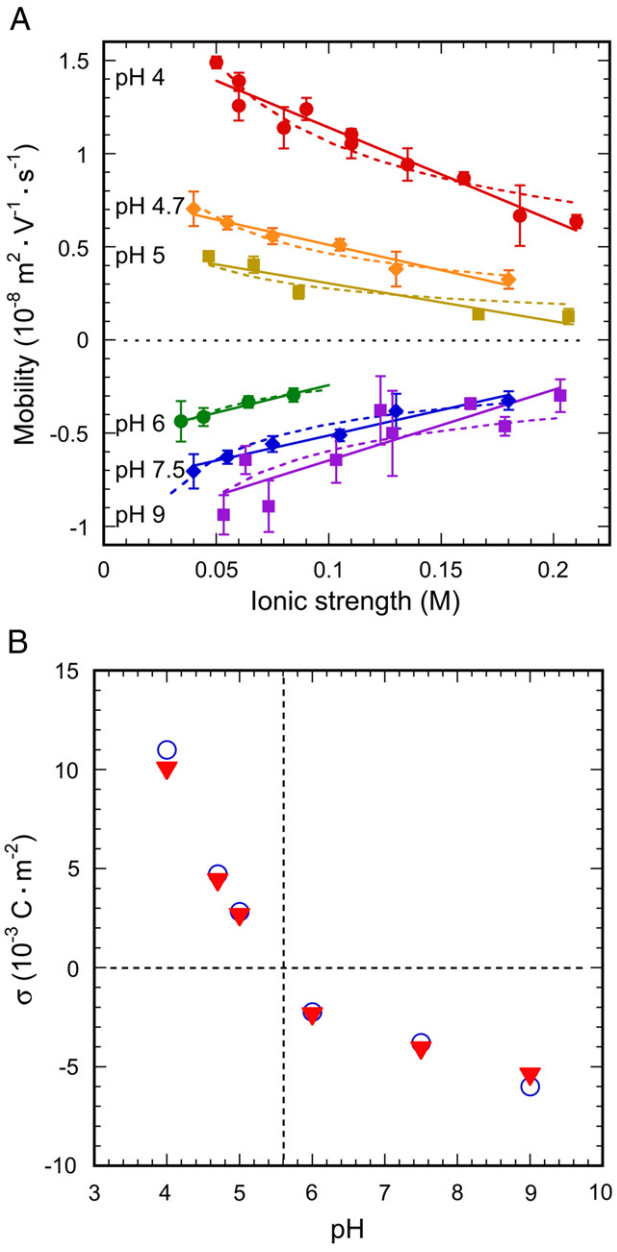

Fig. 4. A. Ionic strength dependence of mobility of SR vesicles at pH 4.0, 4.7, 5, 6.0, 7.5, and 9.0. The solid lines show the linear regression used to obtain the representative mobility values at ionic strength of 0.1 M. The broken curves illustrate the predictions of the mobility from the least squares fit of the Helmholtz–Smoluchowski model. B. Comparison of apparent surface charge density obtained by linear approximation of mobility to 0.1 M (open circles by Method-1), and by the least squares fit of mobility data to Helmholtz–Smoluchowski model (filled triangles by Method-2).

priori known what portion of Ca^{2+}–ATPase is electrophoretically active. Therefore we compute the pH dependence of charges from amino acid sequences for different structural units of Ca^{2+}–ATPase.

Table 1
Bulk pH, interfacial pH, mobility, apparent ζ-potential, and apparent surface charge density of SR vesicles at reference ionic strength of 0.1 M.

pH	pH_{if}	μ, (10^{-8}m^{2}V^{-1} s^{-1})	ζ, (V)	σ, (C-m^{-2})
4.0	4.25	1.14 ± 0.07	$(15.0 \pm 0.9) \times 10^{-3}$	$(11.0 \pm 0.7) \times 10^{-3}$
4.7	4.8	0.51 ± 0.06	$(6.5 \pm 0.7) \times 10^{-3}$	$(4.7 \pm 0.5) \times 10^{-3}$
5.0	5.1	0.30 ± 0.03	$(3.9 \pm 0.4) \times 10^{-3}$	$(2.8 \pm 0.3) \times 10^{-3}$
6.0	5.9	-0.24 ± 0.06	$-(3.1 \pm 0.7) \times 10^{-3}$	$-(2.2 \pm 0.5) \times 10^{-3}$
7.5	7.4	-0.46 ± 0.05	$-(5.8 \pm 0.7) \times 10^{-3}$	$-(4.2 \pm 0.5) \times 10^{-3}$
9.0	8.9	-0.65 ± 0.11	$-(8.3 \pm 1.4) \times 10^{-3}$	$-(6.0 \pm 1.0) \times 10^{-3}$

These are A, P, and N domains, the transmembrane helices M, and the entire Ca^{2+}–ATPase. Of special interest are the charges residing in the cytoplasmic domains A, P, and N. These domains protrude from the outer surface of the SR vesicle and should therefore have a prominent effect on vesicle mobility. This expectation follows from Eq. (5). It is applicable to "large particles" having a charged plane at distance d above the surface of the bilayer [28]. For such a particle the mobility in Debye–Hückel approximation is

$$\mu = \frac{\sigma}{\eta\kappa}[\kappa d + \exp(-\kappa d)]. \quad (5)$$

It is important to recognize that the mobility of such particles is greater than that predicted by the conventional electrokinetic model assuming smeared charge at the physical surface. In case of SR, Eq. (5) can be used as a theoretical guide that indicates that charges extended from the surface have a greater influence on mobility than those directly on the surface.

The ionizable amino acids of the Ca^{2+}–ATPase of rabbit skeletal muscle (known as SERCA1a) were determined from the amino acid sequence given in Fig. 5 in reference [29]. To determine the types and frequencies of occurrence of ionizable amino acids in the cytoplasmic domains of SR vesicles we used the definitions of domains given by Reuter, Hinsen, and Lacapere [30].

The types of ionizable amino acid side chains present in SERCA1a, their number in the corresponding domains, and their pKa's are summarized in Table 2. These data were used to calculate the pH profiles of the charge of the individual segments of Ca^{2+}–ATPase.

In addition to three individual domains: A, P, and N, two other structures were considered. One is the combination domain designated as the APN domain and the other consists of the entire Ca^{2+}–ATPase. The charge of APN domain includes the sum of charges on the A, P, and N domains. The APN domain was included because the A, P, and N domains extend furthest from the surface of the bilayer and constitute a large fraction of the outer surface of SR vesicles [16,20,30]. The entire Ca^{2+}–ATPase was added for comparison.

The pH profiles of the net charge on individual A, P, and N domains and on helices M1–M10 (H domain) are shown in Fig. 6A. It can be seen that domain A is practically uncharged at high pH and becomes positively charged at pH <7. Domain P carries a net negative charge at pH >4.5. Domain N is positively charged at pH <5 and becomes negatively charged at pH >7. Within 5<pH<7 domain N is approximately neutral. In Fig. 6B the pH dependence of charge on the combination APN domain and on the entire Ca^{2+}–ATPase are compared. It is notable that the pH profile of charge on the APN domain and the N domain alone are similar to that of mobility (Fig. 5). The N domain was not selected as the sole origin of mobility of SR vesicles since there is no physically meaningful reason to assume that A and P domains would be electrophoretically inactive. These domains carry significant charge and their charges are also located above the lipid bilayer for which they are expected to enhance the vesicle mobility.

Helices were excluded as a candidate for electrophoretic activity because of the intra-bilayer location ($d = 0$, see Eq. 5), and because of the absence of evidence that negatively charged lipids present in SR membrane are electrophoretically active, as discussed below.

We also considered whole Ca^{2+}–ATPase as the origin of mobility (Fig. 6B). Total charge of Ca^{2+}–ATPase is not a candidate because Ca^{2+}–ATPase acquires a high negative charge above pH 5 and the mobility reversal would occur well below the observed $pH_{rev} = 5.6$.

3.3. The relationship between electrophoretic mobility of SR vesicles and the electric charge of APN domains of Ca^{2+}–ATPase

In this section existence of a direct correlation between the measured electrophoretic mobility of SR vesicles and the electric charge

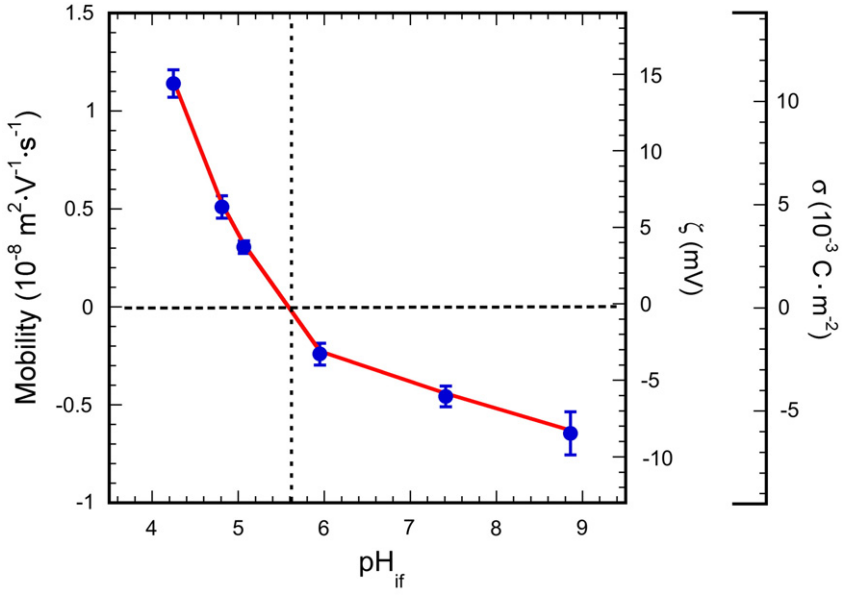

Fig. 5. Experimental values of electrophoretic mobility, apparent ζ-potential, and apparent surface charge density σ as a function of pH at the surface of SR vesicles (pH_{if}). The interfacial pH includes the effect of electrostatic potential on [H^+], Eq. (4). The connecting lines have no theoretical significance. The vertical line indicates the pH of polarity reversal of electrophoretic mobility, $pH_{rev} = 5.6$.

Q_{APN} of APN domain is demonstrated. The correlation is established in Fig. 7 by the linear relationship between the mobility of SR vesicles and the total charge of APN domain. Similar relationships exist between the other electrokinetic quantities of SR vesicles ζ, σ and the charge Q_{APN}. In Fig. 7 the mobility and interfacial pH were taken from Table 1 and the charge of APN domain was computed from amino acid content and interfacial pH using the pKa values given in Table 2.

The straight line Fig. 7 depicts the result of linear regression between the mobility and the charge of APN domain. From the regression equation

$$\mu(pH) = \alpha + \beta Q_{APN}(pH) \quad (6)$$

follows that the optimum slope $\beta_{LSF} = (0.043 \pm 0.002) \times 10^{-8}$ $m^2 V^{-1} s^{-1} e^{-1}$ and the offset $\alpha_{LSF} = (0.16 \pm 0.02) \times 10^{-8}$ $m^2 V^{-1} s^{-1}$. Thus Eq. (6) and the data in Fig. 7 establish the correlation between the mobility of SR vesicles and the charge of APN domain. The value of slope β computed from Helmholtz–Smoluchowski model, β_{HS}, resulting from the combination of Eqs. (2) and (3), yielded a value equal to 30% of the least square fit value β_{LSF}. It indicates that the hydrodynamic friction dominates over the mobility enhancement predicted by Eq. (5).

Note that the regression line in Fig. 7 does not pass through the origin, there is a residual mobility for $Q_{APN} = 0$. This residual mobility determines the value of the offset, α, in the fitting function. The offset originates from errors in the data, the effect of other charges in SR membrane that are electrophoretically active, from incomplete understanding of conditions of ionization of amino acids in APN domain and the mechanism of mobility of SR vesicles.

Whereas Fig. 7 relates the measured mobility to the charge of APN domain, Fig. 8 illustrates the pH dependence of the measured mobility as well as the mobility predicted from Eq. (6). Even though Figs. 7 and 8 are conceptually equivalent, the agreement between the measured mobility and the mobility computed from Eq. (6) confirms the notion that the electrophoretic mobility of SR vesicles originates from charges on APN domains. The advantage of Fig. 8 is that the interfacial pH is displayed on the horizontal axis of the plot as an independent experimental variable, like experimental results in Fig. 5.

Table 2
Amino acid composition of A, P, and N domains, M1–M10 helices, combination APN domain, and total Ca^{2+}–ATPase. The quantities in columns are the name of each amino acid[a]; pKa value, and their number in each domain.

Amino Acid	pKa	A	P	N	M1–M10	APN	Ca^{2+}–ATPase
Arginine	12.5	9	9	15	8	33	43
Aspartic acid	3.9	10	10	14	4	34	50
Cysteine	8.0	1	7	8	6	16	25
Glutamic acid	4.1	12	13	19	15	44	76
Histidine	6.1	4	0	0	1	4	12
Lysine	10.5	13	7	17	8	37	51
Tyrosine	10.1	3	2	5	7	10	21

[a] The amino acid composition of Ca^{2+}–ATPase includes amino acids in links in addition to A, P, N and M domains.

3.4. Why charged lipids of SR membrane do not significantly contribute to mobility of SR

The lipid composition of SR obtained by Waku et al. [31] given in terms of percentage of the total lipid content is as follows: phosphatidylcholine (68.2%), phosphatidylethanolamine (16.8%), phosphatidylinositol (7.6%), phosphatidylserine (2%), sphingomyelin (3.7%) and unidentified lipids (1.7%). According to Narasimhan et al. [32] SR contains 0.613 μg of sialic acid/mg SR protein, which yields about 0.3 mol of sialic acid per mole of Ca^{2+}–ATPase.

Within the pH range of interest, the charge of lipid matrix of SR is dominated by phosphatidylinositol and phosphatidylserine. The contribution of sialic acids is negligible, about −0.3e per unit cell. Using the unit cell areas, 123 nm^2 for tetragonal and 130 nm^2 for hexagonal [21], after subtracting 12.6 nm^2 for the stalk of the Ca^{2+}–ATPase, the lipid bilayer unit cell contains, respectively 3.2 molecules of PS and 12.0 molecules of PI for the tetragonal cell and 3.4 molecules of PS and 12.8 molecules of PI in the hexagonal cell. These estimates were made for 0.7 nm^2 membrane surface area per lipid.

Phosphatidylserine has three protonation/deprotonation sites. Their respective pKa's are 2.6 (R2-HPO4), 5.5 (R-COOH) and 11.55 (R-NH3+). Phosphatidylinositol has one protonation/deprotonation site (R2-HPO4) with pKa = 2.5. The pH dependence of mobility of a vesicle containing the same amount of PS and PI per unit cell area as present in SR membrane is depicted in Fig. 9. If the electrophoretic mobility of SR originated from negatively charged lipids present in SR

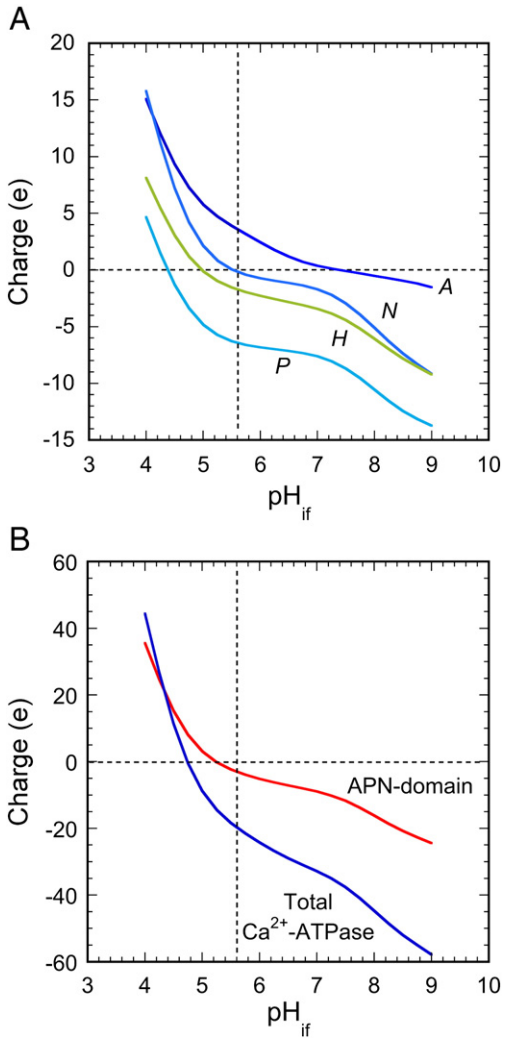

Fig. 6. A. The dependence of the net charge of A, P, and N domains and of M1–M10 helices (H) of the Ca^{2+}–ATPase on interfacial pH. The pH profile was calculated from frequencies of occurrence and pKa values of amino acids given in Table 2. The vertical line indicates the pH of polarity reversal of electrophoretic mobility, $pH_{rev} = 5.6$. B. Comparison of pH dependence of charge on APN domain, Q_{APN}, and that of the charge of the total Ca^{2+}–ATPase, Q_{ATPase}. The vertical line indicates the pH of polarity reversal of electrophoretic mobility, $pH_{rev} = 5.6$. The pH profile was calculated from frequencies of occurrence and pKa values of amino acids given in Table 2. The pH dependencies of charge, Q_{APN} and Q_{ATPase} should be compared with the pH dependence of mobility in Fig. 5.

membrane the pH dependence of mobility of SR vesicle would resemble the mobility plot in Fig. 9. In contrast, the pH dependence of mobility of SR vesicles predicted from the pH-dependent charge of APN domain illustrated in Fig. 8 agrees with the data.

A contribution of charged lipids to mobility of SR vesicles has not been observed. This phenomenon can be understood in terms of the concept that charges above the surface of SR lipid bilayer, such as charges in APN domain, are electrophoretically more active than charges at the surface of the bilayer. The mobility enhancement effect for charges in APN domain follows from Eq. (5) where the expression in square brackets can be defined as the mobility enhancement factor f_d. The existence of mobility enhancement effect was confirmed by studies in McLaughlin's laboratory [28,33,34]. It also follows from Eq.(5) that for lipid vesicles $f_d(\text{lipid}) = 1$ since charged lipid headgroups are at the surface of the bilayer, $d = 0$, and that SR vesicles with charges displaced above the surface of the bilayer have enhancement factor >1.

To evaluate the mobility enhancement effect consider that charges on APN domains can be represented by an equivalent charged plane

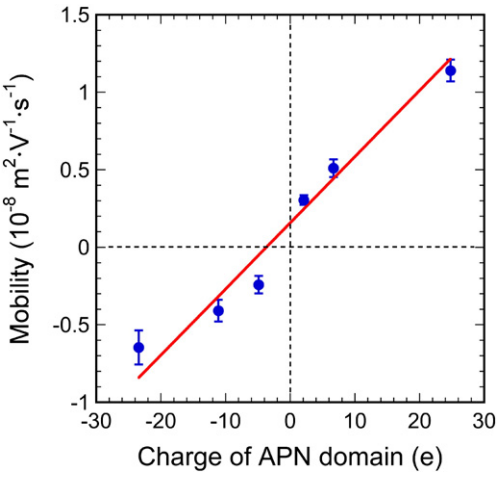

Fig. 7. Demonstration of existence of linear relationship between the mobility and charge of APN domain. The experimental mobility was taken from Fig. 5 and the charge of APN domain from Fig. 6B.

passing through the center of mass of APN domains at distance d_{APN}. For such particles the mobility enhancement factor $f_d(\text{APN}) = \kappa d_{APN} + \exp(-\kappa d_{APN})$. For 0.1 M monovalent salt solution used in our studies the Debye length, $1/\kappa$, is about 0.96 nm. From Toyoshima's diagrams of the conformations of A, P, and N domains during the Ca^{2+} transport cycle, (Fig. 1 in reference [16]) we estimate that the center of mass of the cytoplasmic domains is about 7.5 nm above the bilayer. For a hypothetical charged plane at distance $d_{APN} = 7.5$ nm above the surface of the bilayer the mobility enhancement factor is $f_d(\text{APN}) = 7.8$, i.e. almost one order of magnitude greater than that for the charged bilayer. The above values of f_d are applicable to particles without frictional surface layer.

In contrast to f_d that is applicable to smooth particle, we assign F_d to be the mobility enhancement factor for a particle with hydrodynamic friction layer. The effect of hydrodynamic friction is that, in general, $F_d < f_d$. Due to hydrodynamic friction within the surface layer of SR the contribution of charged lipids to the mobility of SR vesicles is smaller than that for a smooth particle. The magnitude of the mobility enhancement factor originating from the charges displaced from the bilayer (Eq. (5)) is also reduced due to the attenuation of velocity of electroosmotic flow within the frictional layer. These conclusions follow from the solution of Navier–Stokes equation for electroosmotic

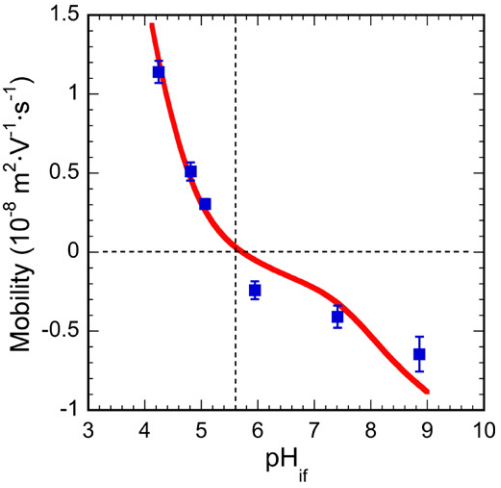

Fig. 8. Plot of mobility of SR vesicles (solid curve) predicted from the pH dependence of the total charge Q_{APN} according to Eq.(6). The squares denote the experimental values of mobility of SR vesicles at ionic strength 0.1 M given in Table 1. The vertical line indicates the pH of polarity reversal of electrophoretic mobility, $pH_{rev} = 5.6$.

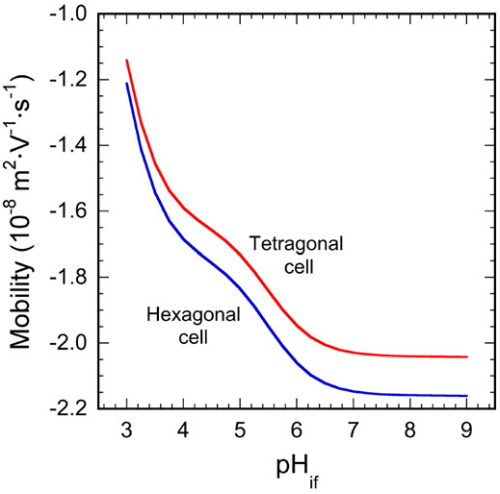

Fig. 9. The pH dependence of mobility of vesicles having the same content of phosphatidylinositol and phosphatidylserine as the lipid bilayer of SR. It was calculated from Helmholtz–Smoluchowski model of mobility using the data on lipid content of SR and the pKa values of protonation/deprotonation sites of lipids given in the text. Unit cell areas are from [21]. The contribution of negatively charged lipids is not observable in the measured pH dependence of mobility of SR vesicles (Fig. 8).

velocity of flow within frictional layers shown in references [19,26,28]. In our opinion, the properties of frictional layers and spatial distribution of charges are the main reasons why the mobility contribution from charged lipids in SR bilayer is not observable in the mobility data.

3.5. Implications of the linear relationship between the mobility of SR vesicles and the charge of APN domain of SR

The charge of APN domain is pH-dependent. At $pH < pH_{rev}$ the net charge of APN domain is positive and it becomes negative at $pH > pH_{rev}$. In spite of the change of charge polarity of the cytoplasmic domains and possible changes in conformations in APN domain the slope of mobility vs. charge shown in Fig. 7 is pH-independent. The value of slope β in Eq. (6), $\beta_{LSF} = (0.043 \pm 0.002) \times 10^{-8}$ $m^2 V^{-1}$ s^{-1} e^{-1}, is valid for the full range of pH values, from pH 4 to pH 9. Since the slope of the mobility for the low and high pH data is the same there appears to be no significant reorganization of membrane surface of SR with pH that would affect the electrophoretic mobility of SR vesicles.

4. Conclusions

The significance of this work is that it demonstrated that the electrophoretically active charge of Ca^{2+}–ATPase are ionizable amino acids of APN domain obtained from the amino acid sequence of SERCA1a Ca^{2+}–ATPase. The experimental pH dependence of mobility was reproduced by the pH dependence of total charge of A, P, and N domains computed using pKa values for their free state in water. The agreement suggests that A, P, and N domains are not compact but possess loose water-penetrable structure. This notion is consistent with results of molecular dynamics simulations demonstrating that A, P, and N domains undergo large conformational changes and movement during the calcium pumping cycle and that the thermal energy can drive these conformational changes. Apparently the conformational barriers are lowest when the cytoplasmic domains are loose and hydrated. Other features of the mobility of SR vesicles are that (a) there is no traceable contribution to mobility of SR vesicles from negatively charged lipids, and (2) the mobility is a linear function of the calculated total charge of cytoplasmic domains of Ca^{2+}–ATPase. The pH-independent constant of proportionality between the charge of APN domain and mobility indicates that the expected hydrodynamic friction produced by the cytoplasmic domains is independent of their charge.

Acknowledgements

We appreciate the support from the Physics Department of Portland State University, and would like to thank Mr. Rod Cruse of Beckman-Coulter and Mr. Leroy Laush of the Portland State University electronic shop for the past and the present maintenance of the electrophoretic mobility analyzer DELSA. We thank Professor P. T. Leung for the discussion of theoretical issues of this project and Professors Rolf Könenkamp and Gertrude Rempfer for the use of the photoelectron microscope for characterization of SR vesicles. This research was partially supported by DOE under grant number DE-FG02-07ER46406 and NSF grant number DBI-0352224.

References

[1] Y. Nakano, K. Makino, H. Ohshima, T. Kondo, Analysis of electrophoretic mobility data for human erythrocytes according to sublayer models, Biophys. Chem. 50 (1994) 249–254.
[2] R. Sonohara, N. Muramatsu, H. Ohshima, T. Kondo, Difference in surface properties between *Escherichia coli* and *Staphylococcus aureus* as revealed by electrophoretic mobility measurements, Biophys. Chem. 55 (1995) 273–277.
[3] Y. Hong, D.G. Brown, Electrostatic behavior of the charge-regulated bacterial surface, Langmuir 24 (2008) 5003–5009.
[4] J.A. Cohen, Electrophoretic characterization of liposomes, Meth. Enzymol. 367 (2003) 148–176.
[5] H. Ohshima, Theory of Colloid and Interfacial Electric Phenomena, Elsevier, 2006.
[6] J. Lyklema, Electrokinetics after Smoluchowski, Colloids Surf., A 222 (2003) 5–14.
[7] S.S. Dukhin, N.M. Semenikhin, Theory of polarization of double layer and its effect on electrokinetic and electrooptic phenomena and dielectric permeability of disperse systems. Calculation of electrophoretic and diffusion-phoretic mobilities of solid spherical particles, Koll. Zhur. 32 (1970) 360–368.
[8] R.W. O'Brien, L.R. White, Electrophoretic mobility of a spheroidal colloidal particle, J. Chem. Soc., Faraday Trans. 2 (74) (1978) 1607–1626.
[9] Y.-C. Kuo, Electrophoresis of a biocolloid covered with a cation-absorptive membrane, J. Phys. Chem. B 109 (2005) 11727–11734.
[10] A.V. Delgado, F. Gonzalez-Caballero, R.J. Hunter, L.K. Koopal, J. Lyklema, Measurement and interpretation of electrokinetic phenomena, Pure Appl. Chem. 77 (2005) 1753–1805.
[11] J.F.L. Duval, H. Ohshima, Electrophoresis of diffuse soft particles, Langmuir 22 (2006) 3533–3546.
[12] R.G. Hill, Hydrodynamics and electrokinetics of spherical liposomes with coatings of terminally anchored poly(ethylene glycol): numerically exact electrokinetics with self-consistent mean-field polymer, Phys. Rev. E 70 (2004) 051406/1–051406/16.
[13] J.J. Lopez-Garcia, C. Grosse, J. Horno, A new generalization of the standard electrokinetic model, J. Phys. Chem. B 111 (2007) 8985–8992.
[14] M.D. Pysher, M.A. Hayes, Examination of the electrophoretic behavior of liposomes, Langmuir 20 (2004) 4369–4375.
[15] M.D. Pysher, M.A. Hayes, Effects of deformability, uneven charge distribution, and multiple moments on biocolloid electrophoretic migration, Langmuir 21 (2005) 3572–3577.
[16] C. Toyoshima, Structural aspects of ion pumping by Ca2+–ATPase of sarcoplasmic reticulum, Arch. Biochem. Biophys. 476 (2008) 3–11.
[17] G.J. Arrio, A. Carrette, J. Chevallier, D. Brethes, Electrokinetic and hydrodynamic properties of sarcoplasmic reticulum vesicles: a study by laser Doppler electrophoresis and quasi-elastic light scattering, Arch. Biochem. Biophys. 228 (1984) 20–229.
[18] D. Brethes, D. Dulon, G. Johannin, B. Arrio, T. Gulik-Krzywicki, J. Chevallier, Study of the electrokinetic properties of reconstituted sarcoplasmic reticulum vesicles, Arch. Biochem. Biophys. 246 (1986) 355–365.
[19] P. Smejtek, M. Mense, R. Word, S. Wang, Electrokinetic properties of the sarcoplasmic reticulum membrane obtained from reconstitution studies, J. Membr. Biol. 167 (1999) 151–163.
[20] C. Toyoshima, M. Nakasako, H. Nomura, H. Ogawa, Crystal structure of the calcium pump of sarcoplasmic reticulum at 2.6 A resolution, Nature 405 (2000) 647–655.
[21] C.A. Napolitano, P. Cooke, K. Segelman, L. Herbette, Organization of calcium pump protein dimers in the isolated sarcoplasmic reticulum membrane, Biophys. J. 42 (1983) 119–125.
[22] D.H. MacLennan, Purification and properties of an adenosine triphosphatase from sarcoplasmic reticulum, J. Biol. Chem. 245 (1970) 4508–4518.
[23] H.M. Kalckar, Differential spectrophotometry of purine compounds by means of specific enzymes. III Studies of the enzymes of purine metabolism, J. Biol. Chem. 167 (1947) 461–475.
[24] C. Peracchia, L. Dux, A.N. Martonosi, Crystallization of intramembrane particles in rabbit sarcoplasmic reticulum vesicles by vanadate, J. Muscle Res. Cell Motil. 5 (1984) 431–442.
[25] R.J. Hunter, Zeta Potential in Colloid Science, Academic Press, 1981.

[26] J.A. Cohen, V.A. Khorosheva, Electrokinetic measurement of hydrodynamic properties of grafted polymer layers on liposome surfaces, Colloids Surf., A 195 (2001) 113–127.
[27] P.B. Bevington, Data Reduction and Error Analysis for the Physical Sciences, McGraw-Hill, New York, 1969.
[28] L. Pasquale, A. Winiski, C. Oliva, G. Vaio, S. McLaughlin, An experimental test of new theoretical models for the electrokinetic properties of biological membranes. The effect of UO2++ and tetracaine on electrophoretic mobility of bilayer membranes and human erythrocytes, J. Gen. Physiol. 88 (1986) 697–718.
[29] X. Shi, M. Chen, P.E. Huvos, P.M.D. Hardwicke, Amino acid sequence of a Ca2+ transporting ATPase from the sarcoplasmic reticulum of the cross-striated part of the abductor muscle of the deep sea scallop: comparison to serca enzymes of other animals, Comp. Biochem. Physiol. B 120 (1998) 359–374.
[30] N. Reuter, K. Hinsen, J.-J. Lacapere, Transconformations of the SERCA1 Ca–ATPase: a normal mode study, Biophys. J. 85 (2003) 2186–2197.
[31] K. Waku, Y. Uda, Y. Nakazawa, Lipid composition in rabbit sarcoplasmic reticulum and occurrence of alkyl ether phospholipids, J. Biochem. (Japan) 69 (1971) 483–491.
[32] R. Narasimhan, R.K. Murray, D.H. MacLennan, Presence of glycosphingolipids in the sarcoplasmic reticulum fraction of rabbit skeletal muscle, FEBS Lett. 43 (1974) 23–26.
[33] R.V. McDaniel, A. McLaughlin, A.P. Winiski, M. Eisenberg, S. McLaughlin, Bilayer membranes containing the ganglioside GM1. Models for electrostatic potentials adjacent to biological membranes, Biochemistry 23 (1984) 4618–4624.
[34] R.V. McDaniel, K.A. Sharp, D.E. Brooks, A.C. McLaughlin, A.P. Winisky, D. Cafiso, S. McLaughlin, Electrokinetic and electrostatic properties of bilayers containing gangliosides GM1, GD1a, or GT. Comparison with a nonlinear theory, Biophys. J. 49 (1986) 741–752.
[35] D.L. Stokes, N.M. Green, Structure and function of the calcium pump, Annu. Rev. Biophys. Biomol. Struct. 32 (2003) 445–468.